

VITESS 3 - Virtual Instrumentation Tool for the European Spallation Source

C Zendler^{1,2}, K Lieutenant^{1,2}, D Nekrassov^{1,2} and M Fromme¹

¹ Helmholtz-Zentrum Berlin für Materialien und Energie GmbH, Hahn-Meitner-Platz 1, 14109 Berlin, Germany

² ESS design update programme, Germany

E-mail: carolin.zendler@helmholtz-berlin.de

Abstract. VITESS is a software widely used for simulation of neutron scattering experiments. Although originally motivated by instrument design for the European Spallation Source, all major neutron sources are available. Existing as well as future instruments on reactor or spallation sources can be designed and optimized, or simulated in a virtual experiment to prepare a measurement, including basic data evaluation. This note gives an overview of the VITESS software concept and usage. New developments are presented, including a 3D visualization of instruments and neutron trajectories, a numerical optimization routine and a parallelization tool allowing to split VITESS simulations on a computer cluster.

1. Introduction

Simulation of neutron scattering instruments is important for the development of new beamlines or update of existing instruments by enabling tests of new ideas and optimization of instrument components prior to construction. It can further be useful to conduct a virtual experiment to prepare a planned measurement, analyzing data obtained by a simulation of the instrument in the foreseen configuration including an adequate description of the sample and detector output. Therefore several software programs have been developed to perform such simulations, many of which are dedicated to a certain type of instruments. The Virtual Instrumentation Tool for the European Spallation Source (VITESS) [1, 2] is one of the most widely used of these programs due to its general applicability and easy handling. Despite its name, all major reactor and spallation neutron sources are provided. A detailed implementation of processes involving polarized neutrons [3] is a particular strength of VITESS compared to most other programs, the most common of which are McStas [4] (which recently added a comparable treatment of polarized neutrons [5]), RESTRAX [6], NISP [7] and IDEAS [8]. VITESS is continuously validated by comparison with simulations from aforementioned other programs as well as against data from real experiments [9–12].

VITESS is an open source software available on the VITESS website [13] for Windows, Linux und Macintosh. It is mainly developed at the Helmholtz-Zentrum Berlin (formerly Hahn-Meitner-Institut) in Germany but also includes contributions made by advanced users from other facilities.

In the following, the concepts upon which the VITESS simulation package is build are described in section 2, before the latest developments regarding physical models and software features are introduced in sections 3 and 4.

39 **2. Software concept and program layout**

40 VITESS uses a Monte Carlo ray-tracing technique in which neutrons are modeled as trajectories
41 travelling from a source through an instrument onto a sample in which they are scattered and
42 thereafter measured in a detector. They are assigned with a weight which corresponds to the
43 intensity of the particular phase space element and makes sure that the flux normalisation
44 throughout the instrument is always correct independent of the number of generated trajectories.
45 This weight is modified at each interaction with an instrument component. Each component
46 is represented by a module coming as a stand-alone executable in the software package. These
47 modules run independently of each other, with each single module reading in neutrons from the
48 previous one and passing them on to the next one. A whole instrument is simulated by running
49 several modules sequentially in a pipe. This is done in packages of 10000 neutrons such that in
50 a simulation with larger statistics as usual, all modules can run simultaneously. The properties
51 of generated neutron trajectories can be examined by monitors at any point in the instrument,
52 or written to a file to be read in again later by a new simulation continuing the instrument.

53 VITESS contains a graphical user interface (GUI) from which an instrument can easily be
54 build by assembling the needed modules and which allows to perform complex simulations
55 without knowledge of any scripting language. A VITESS simulation can however also be run
56 either directly from the command line or via a shell, python, perl or tcl script to which an
57 instrument description can be exported from the GUI. This can also be used to run VITESS on
58 a computer cluster, and since release 3.1, a framework is provided to split the simulation on a
59 cluster into several instances to save simulation time.

60 Different kind of neutrons can be studied separately by ray-tracing, which is done by selecting
61 the neutrons of interest in a first run of the simulation and save them into a file, followed by a
62 second simulation in which only those neutrons are processed. Monitor outputs like phase space
63 diagrams or wavelength spectra are written as ASCII files which can be viewed directly from
64 the GUI or analyzed with a preferred external software. A visualization of the neutron paths
65 through the instrument is possible since release 3.0 and is described in more detail in section 4.1.

66 The effect of gravity is included in all components apart from the bender module, but can
67 be switched off if the user sees this fit for a particular purpose.

68 VITESS provides tools to assist the users in performing a simulation by e.g. creating input
69 files or calculating chopper phases. Documentation of all tools and modules as well as of the
70 most important features can be accessed by a help button directly from the GUI, while short
71 descriptions of each parameter of a module can be viewed by clicking on the parameter name.
72 Running a simulation creates a log file in which the pipe command, the module parameters as
73 well as the flux at the end of each module are documented for error diagnostics or later reference.

74 **3. Improved modelling of physics processes**

75 In VITESS 3, the description of physics processes or resulting behavior like emitted source
76 spectra or reflectivity curves has been improved in several modules. This section summarizes
77 the software development connected to a more realistic modelling, while improvements in the
78 program's usage are described in section 4.

79 *3.1. Neutron sources*

80 The description of several sources has been updated, including e.g. new source characteristics
81 of the FRMII reactor in Munich, Germany, and a new source module describing the CSNS
82 spallation source in Dongguan, China. For the spallation neutron sources SNS and ESS, a
83 choice between different moderator descriptions is now available.

84 *3.2. Reflectometer sample*

85 The reflectometer sample module was updated to include both the incoherent and offspecular
 86 scattering. The incoherent scattering probability p is calculated taking into account the inverse
 87 of the mean free path in the sample material μ provided by the user and the randomly chosen
 88 penetration depth of the trajectory in the corresponding sample x : $p = 1 - e^{-\mu x}$. The offspecular
 89 reflectivity mode can be used by providing a lookup table, which contains the reflectivity
 90 $R(k_{z,i}, k_{z,f})$ as a function of the incoming wave vector $k_{z,i} = 2\pi/\lambda \cdot \sin\theta_i$ and the outgoing
 91 wave vector $k_{z,f} = 2\pi/\lambda \cdot \sin\theta_f$.

92 *3.3. Supermirror reflectivity and attenuation models*

93 In VITESS 3, improved models describing the reflectivity of neutrons at supermirror coated
 94 plates as well as in case of no reflection their attenuation in the substrate material are
 95 implemented.

Before VITESS 3, the reflectivity of supermirrors was modelled as a linear decrease from R_0 at the critical angle θ_C corresponding to a mirror coating $m=1$ to a reflectivity value of R_m at $\theta_m = m\theta_C$, followed by an instantaneous drop to zero for $\theta > \theta_m$ in the `sm_ensemble` module, which describes an arbitrary configuration of flat supermirror plates. Parameters R_m , θ_C and θ_m had to be given by the user. Reflectivity files used in the modules `guide` and `bender` allowed for a slower decrease broadened by a factor $W \neq 0$:

$$R = \frac{1}{2}R_0 \left(1 - \tanh \left(\frac{Q - mQ_C}{W} \right) \right) (1 - a(Q - Q_C)) , \quad (1)$$

with $a = \frac{R_m - R_0}{mQ_C - Q_C}$ and $Q_C = 4\pi/\lambda \cdot \sin\theta_C$. The linear reflectivity decrease is however a simplification of the behavior seen in measurements of reflectivity curves of supermirror plates, therefore this model has now been extended by an additional term:

$$R = \frac{1}{2}R_0 \left(1 - \tanh \left(\frac{Q - m_2Q_C}{W} \right) \right) (1 - a(Q - Q_C) + b(Q - Q_C)^2) , \quad (2)$$

96 where W , a , b and m_2 are linear functions of the mirror coating m^1 , which is now the only input
 97 parameter required. Parameters of the new models have been found by fits to experimental
 98 data performed by H. Jacobsen for McStas, and implemented in VITESS within comparison of
 99 simulation results in [12]. The possibility to give W , a , b and m_2 as input parameters is planned
 100 for VITESS version 3.2.

101 In the tool `Generate Mirror Files`, this new model is used in VITESS version 3.0 or newer
 102 if *quadratic Swiss Neutronics description* is chosen. In the `sm_ensemble` module it is default from
 103 VITESS version 3.1 onwards, in which R_0 is also set to $R_0 = 0.99$ instead of formerly $R_0 = 1$.
 104 The reflectivity curves obtained with equation 2 for 1 Å neutrons are shown in figure 1(a) for
 105 m -values between 2 and 6. Table 1 summarizes which model is used in different VITESS versions.

R formula	VITESS version		
	<3.0	3.0	3.1
<code>Generate Mirror Files</code>	1	1, 2	1, 2
<code>sm_ensemble</code>	1	1	2

Table 1. Overview of reflectivity models implemented in different VITESS versions.

¹ $W = -0.0002 \cdot m + 0.0022$; $a = 0.1204 \cdot m + 5.0944$ if $m > 3$, else $a = m$; $b = -7.6251 \cdot m + 68.1137$ if $m > 3$, else $b = 0$; $m_2 = 0.9853 \cdot m + 0.1978$

In the `sm_ensemble` module, neutrons that are not reflected can be transmitted with probability

$$p = e^{-(\mu\lambda + \mu_{ic})d'} , \quad (3)$$

where μ (μ_{ic}) is the wavelength dependent (independent) part of the macroscopic attenuation and d' the pathlength of the neutron trajectory in the mirror, taking refraction into account. An improved description of the attenuation in sapphire is obtained by using

$$p_{Al_2O_3} = e^{-(\mu\lambda + \mu_{ic}/\lambda - c)d'} \quad (4)$$

106 instead of (3), where the constant c was again found by fitting this model to experimental data
 107 in context of the McStas study [12]. Since the aforementioned study uses a mirror on sapphire
 108 substrate, an additional fit of the attenuation for silicon to data extracted from [14] has been
 109 performed for VITESS. The obtained attenuation is shown in figure 1(b) for three different
 110 wavelengths.

111 The old description of equation 3 can still be used by choosing neither silicon nor sapphire
 112 as mirror substrate (option “*other*”).

113 3.4. Neutron detection

114 3.4.1. *Detector geometry and output file* The upgraded `detector` module implemented in
 115 VITESS 3.1 allows for more flexible geometries: instead of a 2D flat detector surface, a 3D volume
 116 detector can be build including several detection layers and a possibly non-perfect resolution in
 117 all three dimension. The overall shape of a detector module can either be “flat” (now meaning
 118 cubic) or cylindrical. A flat detector can now also be simulated with a substructure of detector
 119 tubes. The tube length is equal to either the detector height or width, and a tube geometry
 120 can be chosen with either circular or rectangular tube cross-sections. The different amount of
 121 detection material depending on the neutron position with respect to the center of a circular tube
 122 is taken into account. Space between circular tubes as well as tube walls are treated as vacuum,
 123 i.e. no detection is possible in these regions but also no unwanted scattering is simulated².
 124 Layers can be shifted with respect to each other by half the tube diameter in order to minimize
 125 dead detector regions, as illustrated in the central picture of figure 2(a). The tube option is only
 126 available for an overall flat geometry.

127 In an overall cylindrical geometry, the cylinder axis can now be oriented along all three
 128 coordinate axes. Furthermore, the new `const. phi` option allows the pixel size in the dimension
 129 along the cylinder axis to be variable such that a constant angular width is covered by each
 130 pixel.

131 Several detector modules can be combined in an `array` to build any complex shape.
 132 Figure 2(b) shows an example consisting of two cylindrical and two flat detector modules.

133 An event mode detector output is written if a file name is given as `Output filename`. It
 134 contains a list of detected neutrons with their respective detected position and time as well as
 135 neutron weight and color.

3.4.2. *Detection efficiency and resolution* The efficiency of neutron detection in the `detector`
 module of VITESS version 3.1 can be calculated from the total cross-section σ of neutron
 scattering with the chosen active detector material, a linear approximation of which has been
 extracted from cross-section tables from the National Nuclear Data Center [15] for ³He, ¹⁰B and
⁶Li. For BF₃ or ³He gas, the gas pressure and temperature have to be given as input parameters

²Scattering from e.g. detector housing is not implemented in the `detector` module. However, background
 from a material layer between sample and detection material can be modelled by using the `sample_environment`
 module.

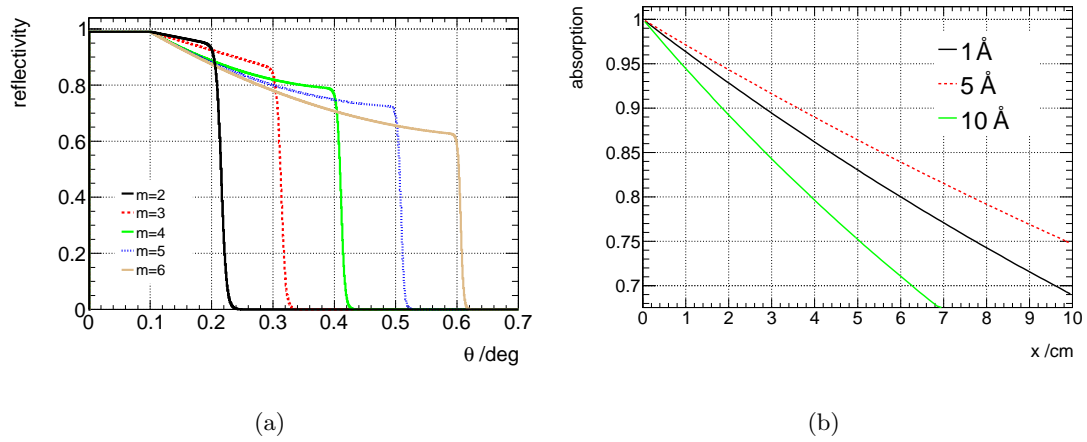


Figure 1. Reflectivity for $\lambda = 1 \text{ \AA}$ neutrons as a function of the scattering angle θ for different super-mirror coatings m as calculated with the new reflectivity model (a) and attenuation in silicon as a function of penetration depth for $\lambda = 1 \text{ \AA}$, 5 \AA and 10 \AA (b).

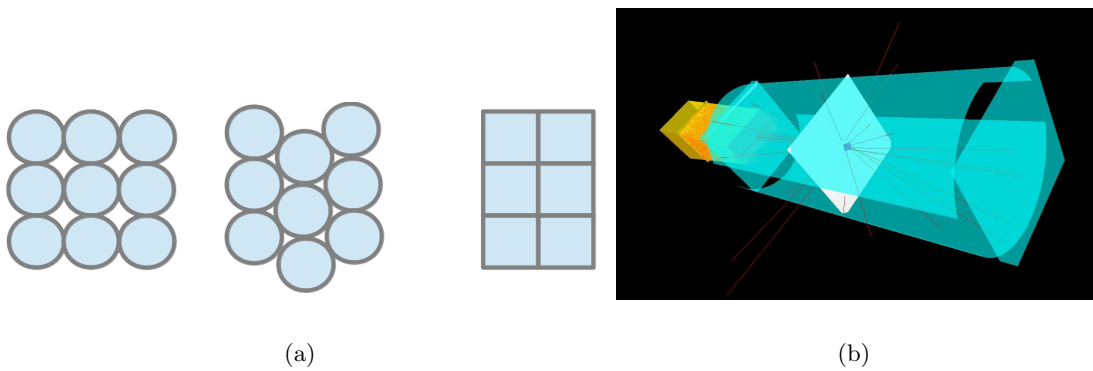


Figure 2. Side view of tube detector with circular, circular shifted or rectangular tubes (a) and detector array consisting of four detector modules (b).

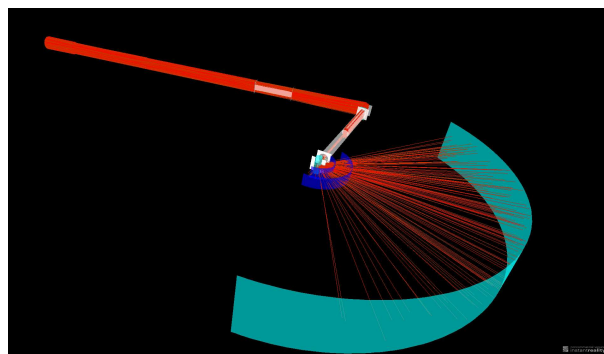


Figure 3. Visualization of the ODIN beamline at IFE, Norway.

from which the particle density N is calculated. For layers of solid material containing ^{10}B or ^6Li , the particle density has to be given directly. The probability of a neutron interaction with the detector material is then calculated as

$$p = N\sigma \cdot e^{-N\sigma l} \cdot L/N_{rep} \cdot \epsilon_{mod} , \quad (5)$$

where L is the detector thickness in the direction along the neutron trajectory and l a random number between zero and L determining the path length of the neutron in the detector before scattering. Every neutron trajectory is split into N_{rep} neutrons detected at different possible path lengths l in the detector material, with the number of repetitions N_{rep} given as input parameter by the user. Compared to sampling the depth l directly from an exponential decay, this approach follows the VITESS philosophy of generating possible outcomes with the same probability and adjusting the weight accordingly to ensure that the tails of the probability distributions are sufficiently populated. The normalization factor L/N_{rep} can be interpreted as a length segment in which the interaction probability is constant, hence the calculated efficiency is more accurate for large $N_{rep} > 1$. Finally, the detection probability can be modified by the wavelength independent input parameter ϵ_{mod} which can represent e.g. losses due to secondary particle detection after neutron scattering in a solid ^{10}B or ^6Li converter layer.

Alternatively, by not choosing a defined detection material (“*other*”), the **efficiency modifier** ϵ_{mod} can be used as a mean detection efficiency of neutrons traversing the detector perpendicular to the detector surface. In this case the detection probability is wavelength independent.

As a third alternative, the detection efficiency can be set by the user via an input file containing the efficiencies for different neutron wavelengths. The probability of neutron detection is then independent of the path through the detector and the exact detector geometry.

The new module further uses 3D pixelization allowing the cloud of charge carriers to be detected in the wrong pixel by the new input parameters `hor.resolution`, `vert.resolution` and `resolution in x`. If one of these parameters is set to a value $\neq 0$, the respective coordinate of the neutron position is changed to a Gaussian random number centered around the true position with width `resolution`. Shifting the output position to the closest pixel center is performed after this Gaussian smear. In case of a tube detector, a non-zero resolution is only allowed in the dimension along the tube axes.

162 4. New or improved program features

163 4.1. Visualization of instruments and neutron trajectories

164 A visualization of the instrument including neutron trajectories can be called from the GUI
165 by the new **Trajectories** button. A prerequisite is an X3D viewer like the recommended
166 **instantreality**. The visualization of the instrument ODIN at IFE, Norway as obtained with
167 the **instantreality viewer** is shown in figure 3 as example.

168 The information about the location and type of interaction of neutron trajectories used for
169 their visualisation can also be utilized to monitor the intensity loss and thus radiation along
170 the instrument, e.g. in a neutron guide. This constitutes the first step towards a background
171 estimation via an interface to a program that models the interaction of radiation and high energy
172 particles with matter.

173 4.2. Numerical Optimization

174 The combination of VITESS simulations with an optimization routine is done such that the
175 latter is the main program and calls the simulation in a subroutine. All files necessary to
176 run a VITESS optimization can be found in the directory `vitess/OPTIMIZATION`, a 7-step
177 recipe is available in `vitess/Concepts/Optimization.pdf`. Three optimization algorithms to

178 choose from are currently implemented: two gradient methods and a metropolis algorithm. The
 179 gradient method `opt_grad` determines gradients in the figure of merit by varying a parameter in
 180 variation steps defined by the user. This step size should be small enough to get a good estimate
 181 of the gradient, but large enough to avoid a false result dominated by statistical fluctuations.
 182 The adapted gradient method `opt_grad_mc` is modified in order to be more robust against
 183 statistical fluctuations in Monte Carlo simulations: a parameter is changed only if variation in
 184 both directions indicate the same gradient, and the step size is varied during the optimization.
 185 The `metropolis` algorithm searches the parameter space in a step size set by the user, accepting
 186 a new parameter value always if the figure of merit is improved, and if it is worse with a
 187 probability according to a kind of Boltzmann factor with a user-defined standard deviation of
 188 the measurement as temperature equivalent. Compared to gradient methods, the `metropolis`
 189 algorithm is less prone to deliver a local optimum, but more simulation steps are needed.

190 The default mapping between optimization parameters p_{opt} and simulation parameters p_{sim}
 191 is a direct assignment: $p_{opt} = p_{sim}$. Other relations can be set by writing a dedicated function;
 192 this procedure is planned to be made more user-friendly in future VITESS versions.

The figure of merit is designed flexible: It is calculated from a signal file containing neutron
 intensity values $I_{sign,i}$, like e.g. a monitor file recording neutrons with a certain divergence at
 the sample position, as

$$FoM = \frac{\sum_i \frac{w_i I_{sign,i} \lambda_i^l}{I_{ref,i}^m}}{\sum_i I_{noise,i}^n}, \text{ or } FoM = \frac{\langle \frac{w_i I_{sign,i} \lambda_i^l}{I_{ref,i}^m} \rangle}{\langle I_{noise,i}^n \rangle}. \quad (6)$$

193 All parameters apart from $I_{sign,i}$ are optional. The powers l , m and n can be float values. The
 194 parameters $I_{ref,i}$, $I_{noise,i}$ and w_i can be given via names of a reference, noise or weight file,
 195 where the former two are like the signal file created as output of the simulation and the latter
 196 is provided by the user. In order to optimize for example the integrated flux at the sample
 197 position, the sum in the figure of merit is chosen, an according monitor file has to be given as
 198 signal file, $l = m = n = 0$ and the reference, noise and weight file are set to `no_file`. If equation
 199 6 is not appropriate, the figure of merit can also be calculated by a user-defined function.

200 4.3. Parallel processing

201 Until VITESS version 3.1, parallel processing was only possible via so-called helper threads using
 202 several cores of the same computer [16]. With the most recent VITESS release, simulations can
 203 be split into several instances on a computer cluster by calling `vitess/TOOLS/gridrun`. The
 204 simulation is then divided into several pipes with less statistics, each of which is sent to the
 205 cluster by either SGE or ssh. A work directory is created in which all input files are copied, as
 206 well as subdirectories for each pipe in which the simulation results are stored. After completion
 207 of all simulations, the output files can be merged and the subdirectories are deleted.

208 4.4. Further improvements

209 New generic monitors `monitor1D` and `monitor2D` can be used to view any neutron parameter,
 210 and combine any two parameters in the latter. Furthermore, two filter parameters can freely be
 211 chosen and combined with a logical AND or OR. The `monitor1D` can create up to three monitor
 212 output files per module (to which the same filter settings are applied). These new generic
 213 monitor modules are planned to replace the sum of old monitor modules, but all are available
 214 for a transition period in VITESS 3. In the old one-dimensional monitor modules, the option
 215 `all_files [yes/no]` has even been added which allows to create a separate monitor output
 216 file for each color present in the neutron beam. The use of color has been changed such that the
 217 value 0 is the default color value and -1 stands for all colors.

218 A new brilliance monitor `mon_brilliance` is available that writes the brilliance instead of the
219 intensity. It can also monitor the brilliance transfer if a `reference file` is given, and calculates
220 the average and peak brilliance which can be written into a `flux file` (but can also be found
221 in the logfile).

222 A new guide module called `guide_ideal` was written to describe guides with a perfect elliptic
223 shape without the use of segmentation. The location of reflection points of neutron trajectories
224 off the guide walls is calculated analytically. The module runs significantly faster compared to
225 the regular guide module with a fine segmentation.

226 Creating a `sm_ensemble` input file is made easier by the new tool `Generate Extraction`
227 `System` in which position and orientation of supermirror plates can be given in a user-friendly,
228 intuitive way. Although written with a bi-spectral extraction system in mind that consists
229 of several stacked and bended mirror plates, this tool can be used for any configuration of
230 supermirrors.

231 In the monochromator module `monochr_analyzer`, a transition mode has been added so the
232 transmitted neutron beam can be analyzed alternatively to the reflected neutrons.

233 The module `writeout` has been expanded such that trajectories can now be written in
234 McStas format, and supplemented by a new module `read_in` that can read trajectories from
235 both VITESS and McStas output files.

236 Handling of the graphical user interface has further been improved: It is now possible to
237 import an instrument description from a file containing the pipe command, to give modules a
238 short descriptive name that appears in the module list to ease distinguishing between similar
239 instrument components, and to select between different programs (gnuplot, shell) with which
240 monitor files are viewed directly from the GUI.

241 Note that only the most important program improvements could be mentioned here; a
242 complete list can be found in the release notes separately available for every VITESS release.
243 Detailed descriptions of new and old features are further available in the documentation within
244 the VITESS software package.

245 5. Summary

246 The software package VITESS is an important tool for the simulation of neutron scattering
247 instruments. It is easy to use due to its graphical user interface, the flexible modular design
248 as well as user-friendly components and tools. The program is under constant development
249 and has made large progress in releases 3.0 and 3.1. New sources have been added and
250 existing moderator descriptions updated, the reflectometer sample can simulate off-specular
251 scattering and incoherent background, and more accurate reflectivity and attenuation models
252 are used in neutron guides and supermirror plates. The detector module has been updated
253 such that it allows more flexible geometries including an array of several detector banks, the
254 detection efficiency can be calculated from the scattering cross-section of a chosen material and
255 resolution effects can be taken into account. Visualization of the simulated instrument including
256 neutron trajectories is now possible. A numerical optimization routine is provided to optimize
257 instruments with respect to a flexibly designed figure of merit. Furthermore, parallel processing
258 on a computer cluster is enabled to save simulation time. Several smaller improvements and
259 new features further ensure VITESS staying a state-of-the-art program contributing to the
260 development of cutting-edge neutron instrument design.

261 Acknowledgments

262 We thank A. Houben for contributions to the `detector` module update. We are further
263 indebted to H. Jacobsen for sharing his reflectivity and attenuation model and comparing McStas
264 simulation results to VITESS.

265 This work was funded by the German BMBF under “Mitwirkung der Zentren der Helmholtz
266 Gemeinschaft und der Technischen Universität München an der Design-Update Phase der ESS,
267 Förderkennzeichen 05E10CB1”.

268 References

- 269 [1] Lieutenant K, Zsigmond G, Manoshin S, Fromme M, Bordallo H N, Champion D, Peters J
270 and Mezei F 2004 **Proc. SPIE** **5536** 134–145
- 271 [2] Zsigmond G, Lieutenant K and Mezei F 2002 *Neutron News* **13** 11–14
- 272 [3] Manoshin S and Ioffe A 2008 *Nucl. Instrum. Meth. A* **586** 81 – 85 proceedings of the
273 European Workshop on Neutron Optics - NOP '07
- 274 [4] Willendrup P, Farhi E, Knudsen E, Filges U and Lefmann K 2014 *Journal of Neutron*
275 *Research* **17** 35–43
- 276 [5] Knudsen E, Tranum-Rømer A, Christiansen P, Willendrup P and Lefmann K 2014 *Journal*
277 *of Neutron Research* **17** 27–34
- 278 [6] Saroun J and Kulda J 1997 *Physica B* **234-236** 1102–1104 proceedings of the First
279 European Conference on Neutron Scattering
- 280 [7] Seeger P A and Daemen L L 2004 *Proc. SPIE* **5536** 109–123
- 281 [8] Lee W T, Wang X L, Robertson J, Klose F and Rehm C 2002 *Applied Physics A: Materials*
282 *Science & Processing* **74**(0) s1502–s1504
- 283 [9] Seeger P, Daemon L, Farhi E, Lee W, Wang X, Passell L, Saroun J and Zsigmond G 2002
284 *Neutron News* **13** 24–29
- 285 [10] Filges U, Saroun J, Juranyi F and Zsigmond G 2006 Presentation at the
286 International Workshop on Applications of Advanced MC simulation URL
287 http://lns00.psi.ch/mcworkshop/papers/focus_intercomparison.pdf
- 288 [11] Klenø K H, Lieutenant K, Andersen K H and Lefmann K 2012 *Nucl. Instrum. Meth. A*
289 **696** 75 – 84 ISSN 0168-9002
- 290 [12] Jacobsen H, Lieutenant K, Zendler C and Lefmann K 2013 *Nucl. Instrum. Meth. A* **717** 69
291 – 76 ISSN 0168-9002
- 292 [13] <http://www.helmholtz-berlin.de/vitess> vitess website
- 293 [14] Freund A K 1983 *Nucl. Instrum. Meth. A* **213** 495 – 501 ISSN 0167-5087
- 294 [15] <http://www.nndc.bnl.gov/sigma/index.jsp?as=10&lib=endfb7.1&nsup=10> national Nu-
295 clear Data Center
- 296 [16] Lieutenant K, Zendler C, Manoshin S, Fromme M, Houben A and Nekrassov D 2013 *Journal*
297 *of Neutron Research* Doi:10.3233/JNR-130005